УДК 616.036.21+616.24-002.17+616-073.756.8-053.84
http://dx.doi.org/10.22328/2079-5343-2023-14-4-73-81

ASSESSMENT OF PULMONARY FIBROSIS SEVERITY AT AUTOPSY IN PATIENTS AFTER COVID-19: COMPARISON WITH QUANTITATIVE CT SCAN DATA IN THE ACUTE PHASE OF THE DISEASE

[1,3]Anna V. Zakharova[*], *[2]Anton N. Gvozdetskiy*, *[4]Dmitry A. Alekseev*, *[1]Alexander V. Pozdnyakov*
[1]St. Petersburg State Pediatric Medical University, St. Petersburg, Russia
[2]North-Western State Medical University named after I. I. Mechnikov, St. Petersburg, Russia
[3]City Multidisciplinary Hospital No. 2, St. Petersburg, Russia
[4]City pathology department, St. Petersburg, Russia

INTRODUCTION: After the COVID-19 pandemic, there is increasing evidence that many patients show fibrous changes in lung tissue accompanied by functional lung disorders. Objective data on the histopathogenesis of such changes is still insufficient. Prospective studies are required to fully assess the consequences of these clinical manifestations.
OBJECTIVE: Evaluation of the capabilities of digital processing of histological preparations of lung tissue and their comparison with quantitative CT data of lung patients in the acute phase of COVID-19.
MATERIALS AND METHODS: The study included data from patients after COVID-19 (7 women and 3 men aged 47 to 93 years) who died after the acute phase of COVID-19 from extrapulmonary causes. The control group included data from 7 people (5 women and 2 men aged 35 to 93 years) who died shortly after hospitalization from extrapulmonary causes (myocardial infarction or acute cerebral stroke), with no signs of lung diseases, including autopsy results. Digital processing of histological preparations of lung tissue obtained during autopsy was carried out, and their comparison with the results of quantitative semi-automatic processing of CT data.
Statistics. Beta regression (*mgcv* library) was used. The model was characterized by a pseudodetermination coefficient R^2. The association was considered statistically significant at $p<0.05$.
RESULTS: A reliable dependence of the severity of fibrous changes in histological samples on the results of quantitative analysis of CT images of patients in the acute period of COVID-19 was demonstrated.
DISCUSSION: Extrapolation of lung autopsy data through quantitative CT assessment is one of the ways to pre-diagnose and identify groups of patients who require specific treatment of post-COVID-19 pulmonary fibrosis.
CONCLUSION. Computerized digital processing of histological images made it possible to correctly compare the histopathological examination data with the CT picture in COVID-19, which could potentially have a prognostic value in the search for more effective treatment strategies.

KEYWORDS: New coronavirus infection, COVID-19, quantitative computed tomography, post-COVID-19 pulmonary fibrosis, digital morphometry

[*]**For correspondence:** *Anna V. Zakharova, e-mail: ellin-ave@yandex.ru*
For citation: Zakharova A.V., Gvozdetskiy A.N., Alekseev D.A., Pozdnyakov A.V. Assessment of pulmonary fibrosis severity at autopsy in patients after COVID-19: comparison with quantitative CT scan data in the acute phase of the disease // *Diagnostic radiology and radiotherapy.* 2023. Vol. 14, No. 4. P. 73–81, doi: http://dx.doi.org/10.22328/2079-5343-2023-14-4-73-81.

ОЦЕНКА ВЫРАЖЕННОСТИ ЛЕГОЧНОГО ФИБРОЗА ПО ДАННЫМ АУТОПСИИ У РЕКОНВАЛЕСЦЕНТОВ COVID-19: СОПОСТАВЛЕНИЕ С ДАННЫМИ КОЛИЧЕСТВЕННОЙ КТ ЛЕГКИХ В ОСТРОЙ ФАЗЕ ЗАБОЛЕВАНИЯ

[1,3]А. В. Захарова[*], *[2]А. Н. Гвоздецкий*, *[4]Д. А. Алексеев*, *[1]А. В. Поздняков*
[1]Санкт-Петербургский государственный педиатрический медицинский университет, Санкт-Петербург, Россия
[2]Северо-Западный государственный медицинский университет имени И. И. Мечникова, Санкт-Петербург, Россия
[3]Городская многопрофильная больница № 2, Санкт-Петербург, Россия
[4]Городское патологоанатомическое бюро, Санкт-Петербург, Россия

ВВЕДЕНИЕ: После пандемии COVID-19 появляется все больше доказательств того, что у многих реконвалесцентов COVID-19 выявляются фиброзные изменения легочной ткани, сопровождающиеся функциональными нарушениями легких. Объективных данных о гистопатогенезе подобных изменений по-прежнему недостаточно. Для полной оценки последствий этих клинических проявлений требуются проспективные исследования.

ЦЕЛЬ: Оценка возможностей цифровой обработки гистологических препаратов легочной ткани и их сопоставление с данными количественной КТ легких пациентов в острой фазе COVID-19.

МАТЕРИАЛЫ И МЕТОДЫ: В исследование были включены данные пациентов-реконвалесцентов COVID-19 (7 женщин и 3 мужчин в возрасте от 47 до 93 лет), умерших после острой фазы COVID-19 от внелегочных причин. В контрольную группу вошли данные 7 человек (5 женщин и 2 мужчин в возрасте от 35 до 93 лет), умерших вскоре после госпитализации от внелегочных причин (ОКС либо ОНМК), без каких-либо признаков заболеваний легких, в том числе по результатам аутопсии. Проводилась цифровая обработка полученных при аутопсии гистологических препаратов легочной ткани и их сопоставление с результатами количественной полуавтоматической обработки данных СКТ.

Статистика. Использовалась бета-регрессия (библиотека *mgcv*). Модель характеризовалась коэффициентом псевдодетерминации R^2. Ассоциация признавалась статистически значимой при $p<0,05$.

РЕЗУЛЬТАТЫ: Продемонстрирована достоверная зависимость выраженности фиброзных изменений в гистологических образцах от результатов количественного анализа КТ-изображений пациентов в остром периоде COVID-19.

ОБСУЖДЕНИЕ: Экстраполяция данных аутопсийного исследования легких через количественную оценку КТ является одним из способов предварительной диагностики и определения групп пациентов, которым требуется специфическое лечение пост-COVID-19 легочного фиброза.

ЗАКЛЮЧЕНИЕ: Компьютеризированная цифровая обработка гистологических изображений позволила корректно сопоставить данные гистопатологического исследования с КТ-картиной при COVID-19, что потенциально может иметь прогностическое значение в поиске более эффективных стратегий лечения.

КЛЮЧЕВЫЕ СЛОВА: новая коронавирусная инфекция, COVID-19, количественная компьютерная томография, пост-COVID-19 легочный фиброз, цифровая морфометрия

*Для корреспонденции: *Захарова Анна Валерьевна, e-mail: ellin-ave@yandex.ru.*

Для цитирования: Захарова А.В., Гвоздецкий А.Н., Алексеев Д.А., Поздняков А.В. Оценка выраженности легочного фиброза по данным аутопсии у реконвалесцентов COVID-19: сопоставление с данными количественной КТ легких в острой фазе заболевания // *Лучевая диагностика и терапия*. 2023. Т. 14, № 4. С. 73–81, doi: http://dx.doi.org/10.22328/2079-5343-2023-14-4-73-81.

Introduction. The 2019 new coronavirus pandemic (COVID-19) has become one of the most complex public health crises in recent decades. As of December 1, 2022, there have been at least 639 million confirmed cases and 6.6 million deaths [1].

Chest imaging plays an important role in the differential diagnosis, detection of complications, and assessment of prognosis of patients with COVID-19 [2, 3]. Since the early days of the pandemic, radiologists have responded quickly to the emergence of COVID-19 by identifying CT patterns characteristic of COVID pneumonia: ground-glass opacities (GGO), consolidation, reticular lesions (including crazy-paving pattern), reversed halo sign or other symptoms characteristic of organizing pneumonia in the peripheral lung on both sides.

It should be noted that these CT signs may also occur in other diseases, such as influenza pneumonia or cryptogenic organizing pneumonia, therefore it is recommended not to use CT for the diagnosis of COVID-19 as a first line, due to the difficulties of differential diagnosis [4]. However, chest CT is helpful in cases that are difficult to diagnose with PCR test [5]. In addition, chest imaging can detect complications associated with COVID-19, such as pulmonary embolism, attached bacterial pneumonia, and heart failure. This is especially important in case of sudden deterioration in patients with COVID-19 [2, 3, 6] and to determine the severity of pneumonia [7, 8].

Various studies have shown that approximately 70–80% of patients who have recovered from COVID-19 have at least one or more symptoms [9, 10]. The presence of persistent symptoms in COVID-19 reconvalescents has been termed post-COVID syndrome or long-COVID. Given the high volume of cases worldwide, it poses a serious health problem [11]. Prospective studies are required to fully assess the population incidence and consequences of these clinical manifestations.

The most serious complication affecting the respiratory system is post-COVID-19 pulmonary fibrosis [12]. It is characterized by the presence of fibrous changes in the lungs according to CT, associated with functional impairment during follow-up [13, 14]. In a systematic review, post-COVID-19 pulmonary fibrosis was observed in 7.0% of patients [15]. Preliminary data suggest that more than one-third of reconvalescents retain fibrous changes in the early period after COVID-19 [16].

Histologically, pulmonary fibrosis is characterized by the accumulation of extracellular matrix proteins, mesenchymal and immune cells in the intercellular space, which leads to disruption of the normal archi-

tectonics of lung tissue [17]. The main link in the pathogenesis of pulmonary fibrosis is repetitive microdamage of the alveolar epithelium, which leads to an ineffective reparative response and epithelial dysfunction, and subsequently to the activation of collagen-producing cells [13]. Parenchymatous fibrosis leads to thickening of lung tissue [18]. This worsens the functional state of the lungs, reducing the vital capacity (VC) and forced vital capacity (FVC) of the lungs [19]. Post-COVID-19 pulmonary fibrosis can be caused by acute respiratory distress syndrome (ARDS) or directly by pneumonia in the acute period of COVID-19 [20, 21]. In addition, there are risk factors such as advanced age, chronic comorbidities, condition after mechanical ventilation and female gender [20, 22].

Several studies have mentioned screening patients at risk of developing post-COVID-19 pulmonary fibrosis, who underwent pulmonary function tests and chest CT scans to comprehensively evaluate the effects of COVID-19 and to select possible treatment [23–26]. Nevertheless, a number of issues remain unclear — for example, whether fibrotic changes will persist for a long time or may regress, and whether post-COVID-19 pulmonary fibrosis may become progressive as in other interstitial lung diseases. In our opinion, histopathologic studies are of paramount importance in understanding the answer to most of the questions about the features of post-COVID-19 pulmonary fibrosis.

Methods to quantify fibrosis in histological samples are limited [27]. First described as early as 1988, the Ashcroft pulmonary tissue score continues to be used as a method for quantifying the extent of pulmonary fibrosis, despite the subjectivity of assessing changes using this technique [28].

Computerized digital image analysis was developed to assess the severity of fibrosis in various rodent or human tissues, including lung, liver, heart, and kidney [29–33]. In most cases, computerized analysis of digital images assesses the severity of fibrosis by quantifying the content of colored collagen (van Gieson's stain). Quantitative collagen content was estimated by the ratio of the area of stained collagen to the area of analyzed regions of interest selected on the whole slice. The effectiveness of digital processing of histological images was demonstrated by the correlation between lung functional parameters and quantification of fibrosis [27]. We suggested that this approach could be applied to the evaluation of post-COVID-19 pulmonary fibrosis, the severity of which depends on the CT data in the acute period of the disease.

The purpose of this study was to test the possibilities of digital processing of histological preparations of lung tissue and their comparison with quantitative CT data of patients' lungs in the acute phase of COVID-19.

Materials and methods. The study was approved by the local ethics committee of St. Petersburg State Pediatric Medical University, protocol number 31/08, dated October 18, 2023. Informed consent was obtained from each patient.

Clinical material. Autopsy results were obtained at the Vyborg interdistrict centralized pathological anatomical department (a subdivision of the SPb GBUZ «City pathology department»). The study included data from COVID-19 recovalescent patients (10 people) who died from extrapulmonary causes. All patients were previously treated for COVID-19 infection between March 2020 and 2022. Inclusion criteria were (1) positive PCR for COVID-19, (2) COVID-19-typical chest CT scan performed during hospitalization, and (3) absence of clinical, anamnestic, or radiological evidence of other lung diseases (including those detected by autopsy). The period between lung CT and autopsy averaged 5.47 [2.00; 16.01] months. This group included data from 7 women and 3 men, the average age was 78.50 [73.50; 86.75] years. According to the empirical visual scale [34, 35], the severity of COVID-19 manifestations according to CT were as follows: CT-1 (1–24% lung parenchyma involvement) — 6 patients, CT-2 (25–49% involvement) — 3 patients, CT-3 (50–74% involvement) — 1 patient [34].

The control group included data from 7 individuals who died soon after hospital admission from extrapulmonary causes (myocardial infarction or acute cerebral stroke). These patients underwent lung CT at admission according to the standards of care. Inclusion criteria were the absence of clinical, anamnestic or radiologic signs of lung disease, including those detected by autopsy. The period between CT examination and autopsy ranged from 1 to 18 days. This group included 5 women and 2 men; the average age was 74.00 [52.50; 86.00] years.

Chest CT scan. Chest CT was performed on two multidetector CT scanners: Siemens Somatom Definition (64 slices, Siemens Healthineers) and GE Revolution EVO (128 slices, GE Healthcare). All patients underwent chest computed tomography in the supine position, during inhalation (in some cases without breath-holding due to the severity of the patient's condition), without contrast agent injection, with 1.25 mm slice reconstruction. All CT images were viewed by two expert radiologists.

To quantify lung damage in chest CT, the technique described in detail in the article was used [35].

3D lung segmentation with automatic counting of the number of selected pixels was performed using the program Horos 3.3.6[1] (GNU Lesser General Public License, version 3) [35] (Fig. 1).

Further, the classification of Cressoni [36] and Gattinoni was used for quantitative data analysis [37]. Quantitative analysis was performed for each scan in the whole lung volume. The resulting total amount of pixels was estimated in accordance with the above

[1] Horos v3.3.6 https://horosproject.org/.

Fig. 1. Example of automatic lung segmentation in Horos software. The contours of the area of interest are indicated by a black line

Рис. 1. Пример автоматической сегментации легких в программе Horos. Контуры зоны интереса обозначены черной линией

classification. The number of pixels corresponding to unventilated and hypoventilated lung tissue (+100 to −500 HU) indirectly reflected the severity of lung damage.

Preparation of lung tissue samples for morphometry. All autopsies were performed at the Vyborg interdistrict centralized pathological anatomical department (a subdivision of the SPb GBUZ «City pathology department»). The autopsy was performed within 24 hours of death to ensure optimal tissue preservation. General examination and sampling for microscopic examination of the lung was performed by a pathologist.

After visual assessment of the lungs, the most altered tissue sample from each lobe was selected. CT data were not considered when selecting samples. For fixation, tissue samples were soaked in 10% neutral buffered formalin for 48 hours. Next, the tissue was embedded in paraffin, 3 μm thick sections were made and stained with hematoxylin and eosin. For van Gieson's staining of fibrous tissue, slides were deparaffinized and rehydrated to 70% alcohol, incubated for 60 min in Lawson's solution, sequentially treated in 100% and 96% alcohol, washed, stained with Mayer's hematoxylin for 5 min, washed for 5 min, incubated with van Gieson's picrofuchsin for 5 min, and dehydrated in ethanol and xylene with encapsulation under coverslips using polystyrene.

A Nikon Y-TV55 digital microscope was used to examine histological samples in 10 arbitrary fields of view at ×100 magnification.

Using a digital camera, the optical image was converted to a digital image and further morphometry was performed using the recolorize software package in the R v4.3.0 programming language.

Digital morphometry technique. Each image was laid out in RGB color space. After viewing the digital histological images, 12 colors were preset, shown in Fig. 3.

Next, the images were recolorized (i.e., each pixel was assigned the closest color from the palette in

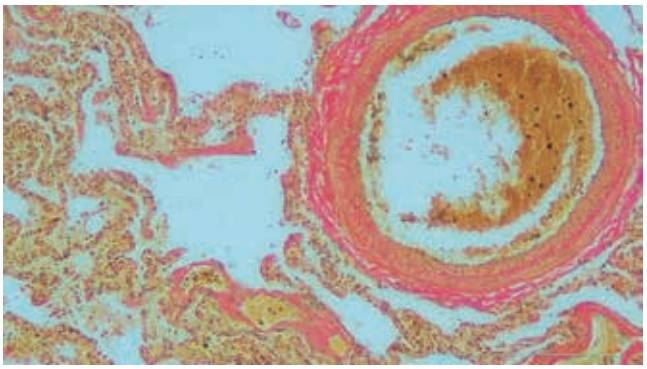

Fig. 2. Example of an original histological image (post-COVID-19). Areas of fibrosis in the lung tissue. Van Gieson's staining, ×100. Van Gieson's staining shows marked perivasal and diffuse fibrosis with areas of lung tissue remodelling as atelectasis and emphysema

Рис. 2. Пример исходного гистологического изображения. Участки фиброза в ткани легкого. Окраска по Ван Гизону, ×100. При окраске по Ван Гизону определяется выраженный перивазальный и диффузный фиброз с участками перестройки легочной ткани в виде ателектазов и эмфиземы

Fig. 3) using the recolorize software package [38]. The colors characterizing lung tissue (palette colors 7 to 11) were selected for further analysis. Palette color 10 corresponded to van Gieson's stained dense connective tissue is enriched in coarse collagenous fibers. An example of recolorization of a digital histological image is shown in Fig. 4.

Fig. 3. Color palette used to analyze digital histological images

Рис. 3. Палитра цветов, использованная для анализа цифровых гистологических изображений

The ratio of the number of pixels corresponding to color 10 of the palette to the sum of pixels corresponding to colors 7–11 of the palette was taken as a quantitative characteristic of pulmonary fibrosis severity.

Statistical analysis. Absolute values and percentage — n (%), were used to describe categorical variables. Discrete variables were described by median, 1–3 quartiles (Md [Q1; Q3]). The *mgcv* library was used for modeling [39]. The proportion of pixels characterizing fibrosis on histological images served as the dependent variable. The group membership (control or COVID-19), the proportion of hypo- and unventilated pixels in CT images, and the logarithm of the proportion of hypo- and unventilated pixels in CT images were used as independent variables. Since the dependent variable belongs to the range (0,1), a beta distribution model was used. The syntax of the model was as described below: *gam(DV~IV, family=betar(), data=df)*. Between-group comparison of

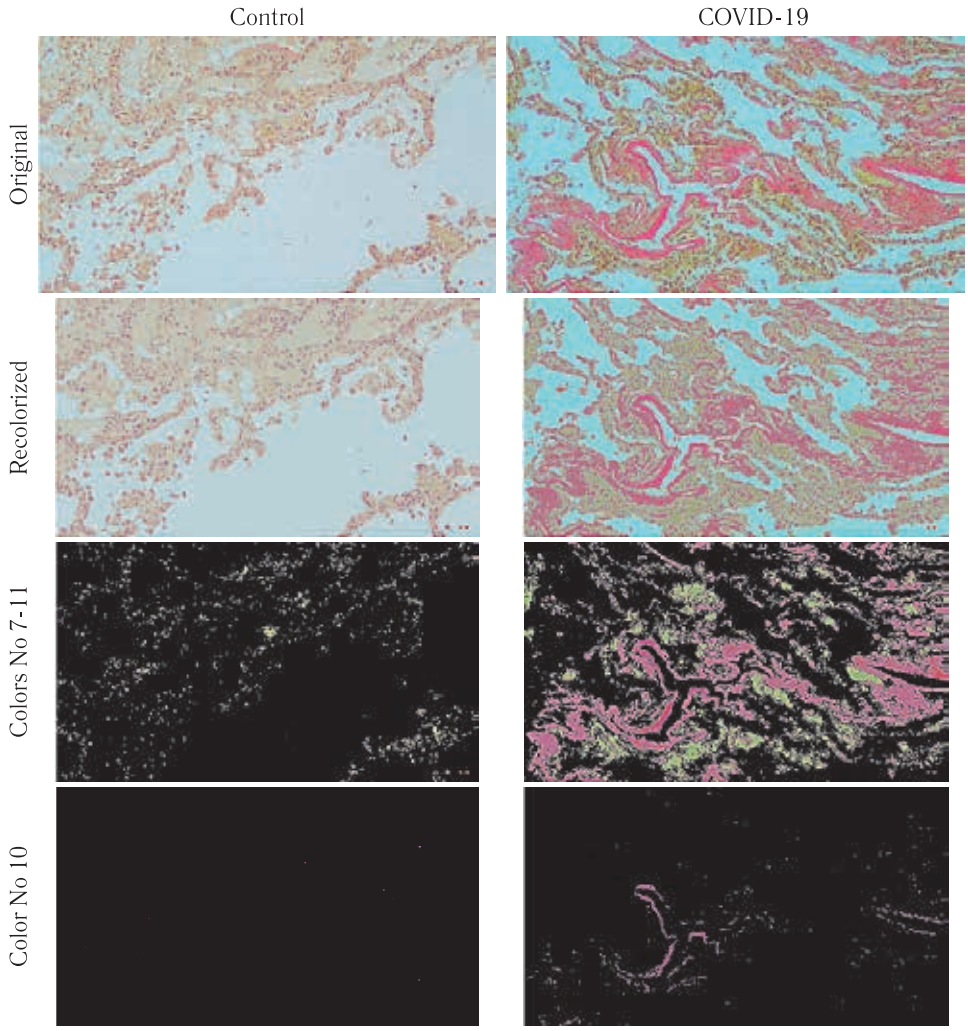

Fig. 4. An example of recolorization of a digital histological image in the COVID-19 group and in the control group
Рис. 4. Пример реколоризации цифрового гистологического изображения в группе «COVID-19» и в группе контроля

the proportions of hypo- and non-hypo-ventilated pixels from CT images was performed similarly.

The model was characterized by a pseudo-determination coefficient R^2. The association was considered statistically significant at $p<0.05$. All calculations are performed in the R v4.3.0 programming language[1].

Results. Quantitative assessment of lung damage in chest CT.

After quantitative processing of the CT images, histograms were obtained for the COVID-19 group and the control group (Fig. 5).

The resulting histograms reflect the highest percentage of unventilated and hypoventilated lung tissue in the COVID-19 group and the lowest in the control group.

Fig. 6 is shown that the proportion of pixels corresponding to unventilated and hypoventilated lung tissue is larger (2.28 (1.22; 4.25), p=0,009) in the COVID-19 group (0.20 [0.15; 0.25]) compared to the control group (0.08 [0.07; 0.16]).

Results of digital morphometry. For each patient, the proportion of pixels corresponding to van Gieson's stained dense connective tissue is enriched in coarse collagenous fibers (equivalent to fibrous tissue) was determined. Fig. 7 shows the ratio of pixel fractions between the COVID-19 and the control groups.

Fig. 7 shows a significantly higher (3.56 (1.71; 7.43), p<0,001) percentage of fibrous tissue in histological samples in patients with COVID-19 (0.76 [0.44; 1.55]%) compared to the control group (0.12 [0.09; 0.20]%).

Three models were constructed to compare the quantitative CT data with the digital morphometry results, and their parameters are summarized in Table.

It follows from Table that group membership (model 1), the proportion of hypo- and unventilated lung tissue (model 2), the logarithm of the proportion of hypo- and unventilated lung tissue (model 3) are statistically significant related to the proportion of pulmonary fibrosis according to digital morphometry. The model 1 had the highest R^2 index, and the Model 3 had a slightly smaller one. Since the predictor in model 3 was a completely digital indicator and did not depend on the subjective asessment of expert physicians, this model was

[1] R Core Team. R. A language and environment for statistical computing. Vienna, Austria: R Foundation for statistical computing, 2023.

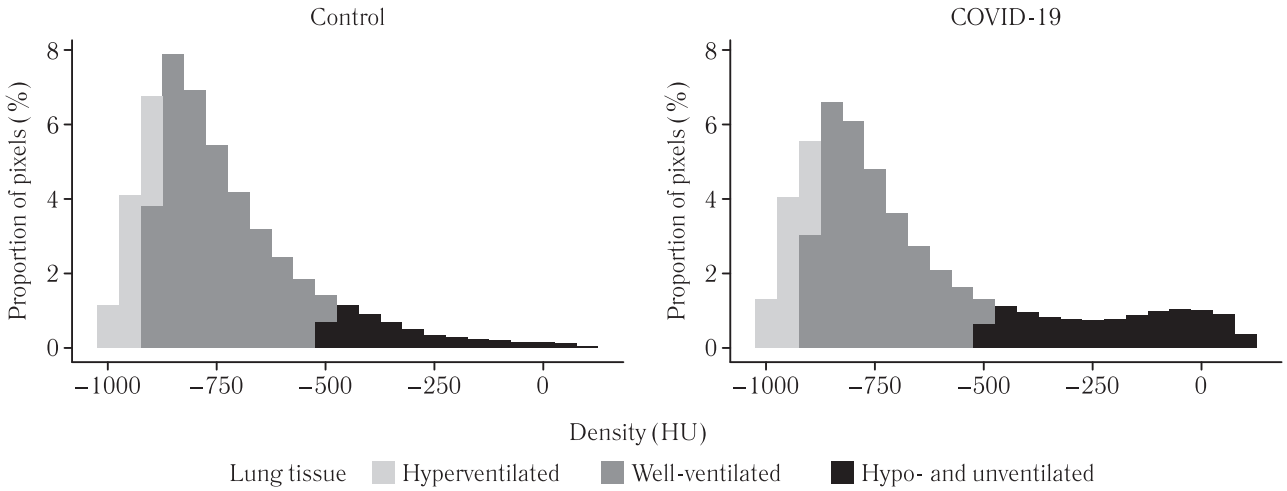

Fig. 5. Distribution of pixel fractions corresponding to unventilated, hypoventilated, well-ventilated, and hyperventilated lung tissue. Explanations are given in the text

Рис. 5. Распределение долей пикселей, соответствующих невентилируемой, гиповентилируемой, хорошо вентилируемой и гипервентилируемой легочной ткани. Пояснения в тексте

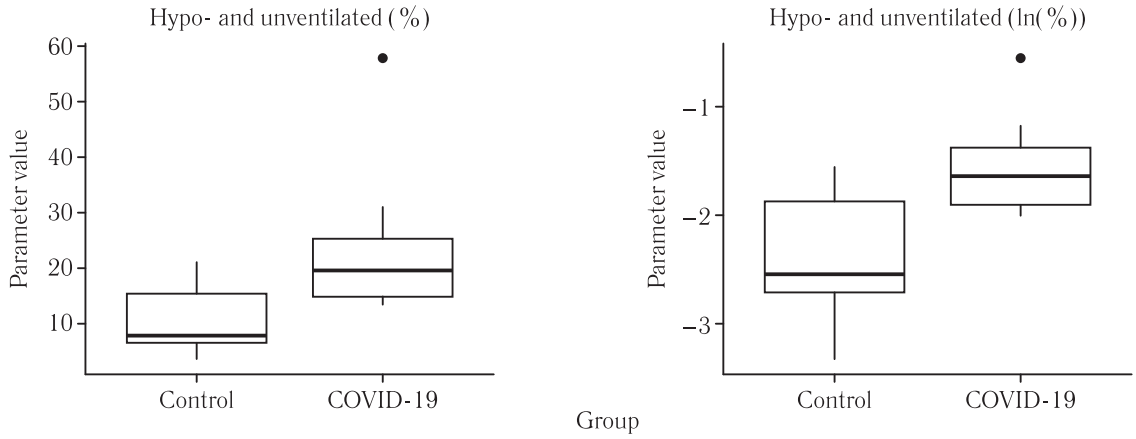

Fig. 6. Graphical representation of the proportions of unventilated and hypoventilated lung tissue according to CT scans of each group

Рис. 6. Графическое представление долей невентилируемой и гиповентилируемой легочной ткани по данным КТ каждой из групп

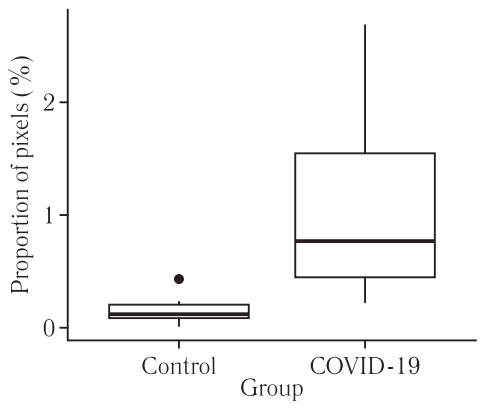

Fig. 7. Distribution of the proportion of fibrous tissue in the COVID-19 group and the control group

Рис. 7. Распределение доли фиброзной ткани в группе «COVID-19» и группе контроля

found to be the best for predicting the severity of pulmonary fibrosis depending on quantitative lung CT data. The graphical representation of Model 3 is shown in figure 8.

Discussion. Clinical practice during the COVID-19 pandemic has shown that chest X-ray plays an important role in the diagnosis of COVID-19 [3] and in the assessment of disease severity [7]. In addition to diagnostic value, CT or radiographic data can be used to assess the prognosis for COVID-19 infection.

In the article by Toussie et al. [40] the severity of lung lesions during chest radiography was an indicator of the risk of hospitalization and intubation of patients. The prognostic value of CT for assessing the functional status of the lungs after the disease has also been shown [26].

The development of quantitative processing of CT images allowed us to build models of pneumonia severity stratification [41, 42], prediction of length of hospital stay and probability of death [43].

The comparison of histological findings with CT imaging is of particular interest to study the pathogenesis of the disease. According to CT data, interstitial collagen deposition accompanied by type II pneumocyte hyperplasia is morphologically detected in the areas of lung

Table

Parameters of comparison of quantitative CT with the results of digital morphometry

Таблица

Параметры сопоставления количественной КТ с результатами цифровой морфометрии

	Model 1	Model 2	Model 3
Constant	0,00 (0,00; 0,01)	0,00 (0,00; 0,01)	0,03 (0,01; 0,07)
Predictor	3,56 (1,71; 7,43)	24,04 (2,52; 229,45)	2,18 (1,28; 3,71)
p-value	<0,001	0,006	0,004
r^2	0,30	0,14	0,26

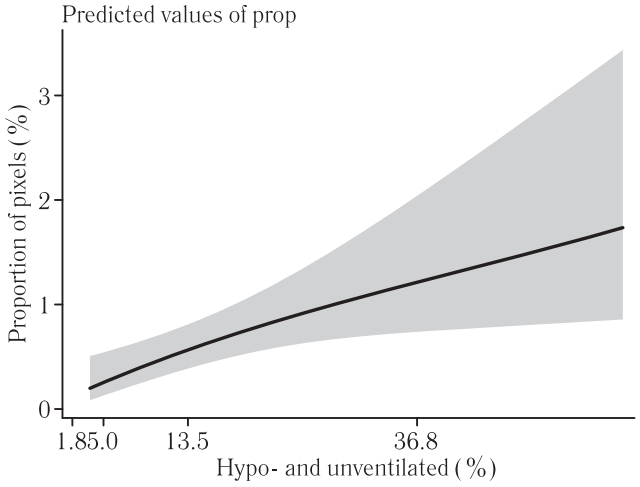

Fig. 8. Graph of dependence of pulmonary fibrosis severity according to digital morphometry on the percentage of hypo- and non-ventilated lung tissue according to quantitative lung CT

Рис. 8. График зависимости выраженности легочного фиброза по данным цифровой морфометрии от процента гипо- и невентилируемой легочной ткани по данным количественной КТ легких

damage [44]. The CT pattern of consolidation and ground-glass opacities (GGO) correlates with numerous pathologic processes, in particular with diffuse alveolar damage, capillary dilation and occlusion, and microthrombosis [45]. In addition, signs of alterations and thrombosis of the pulmonary vessels were found in intact sections of the lungs according to CT data [46].

Despite the inability to display the alveolar-vascular basal membrane on CT images, the ability to stratify the course of the disease is an indirect reflection of ongoing pathologic processes [1]. Since the outcome of alterations is fibrosis [11], it was reasonable to assume that the CT data of the acute phase of COVID-19 would be a predictor of the development of fibrous changes in the lungs.

For the appointment of any method of treatment of post-COVID-19 fibrosis, a preliminary diagnosis is required. The diagnosis of post-COVID pulmonary fibrosis should be based on clinical examination, radiological findings, pulmonary function tests, and pathologic biomarker values [47]. However, the detection of intravital post-COVID-19 fibrosis requires a time-consuming and invasive lung biopsy procedure. For this reason, the mass application of a comprehensive survey is extremely difficult. Extrapolation of autopsy lung examination data through quantitative CT assessment, in our opinion, is one of the ways to pre-diagnose and identify groups of patients who require specific treatment.

This research demonstrates a reliable dependence of the severity of fibrous changes in histological samples with the results of quantitative analysis of CT images of patients in the acute phase of COVID-19. It's crucial for understanding the features of the disease and will increase knowledge of the pathophysiology and consequences of COVID-19.

Conclusion. Thus, in the course of the study it was shown that digital morphometry and quantitative assessment of CT images are useful tools for an objective assessment of the severity of fibrous changes in COVID-19 recovalescents. A reliable dependence of the percentage of fibrous tissue in histological samples on the proportion of pixels characterizing hypo- and non-ventilated lung tissue was shown.

Information about the authors:

Anna V. Zakharova — Assistant Professor of the Department of Medical Biophysics. St Petersburg State Pediatric Medical University, Ministry of Healthcare of the Russian Federation, 194100, Russia, St. Petersburg, Litovskaya Str. 2; Radiologist, Department of Radiology Diagnostics of St. Petersburg State Medical Institution «City Multidisciplinary Hospital No. 2»; 194354, Russia, St. Petersburg, Uchebny lane, 5; e-mail: ellin-ave@yandex.ru; ORCID 0009–0002–6560–6671;

Anton N. Gvozdetskiy — Cand. of Sci. (Med.), Assistant Professor of the Department of Psychiatry, North-Western State Medical University named after I. I. Mechnikov, 191015, Russia, St. Petersburg, Kirochnaya Str, 41; e-mail: comisora@yandex.ru; ORCID 0000–0001–8045–1220;

Dmitry A. Alekseev — Cand. of Sci. (Med.), Head of the department — pathologist of the Vyborg Interdistrict Centralized Pathoanatomical Department (unit of the SPb GBUZ City pathology department); 194354, St. Petersburg, Russia; e-mail: dm_alekseev@bk.ru; ORCID 0000–0001–5912–4663;

Alexander V. Pozdnyakov — Dr. of Sci. (Med.), Professor, Head of the Department of Radiology Diagnostic of St Petersburg State Pediatric Medical University, Ministry of Healthcare of the Russian Federation; 194100, Russia, St. Petersburg, Litovskaya Str, 2; e-mail: pozdnyakovalex@yandex.ru; ORCID 0000–0002–1110–066X.

Сведения об авторах:

Захарова Анна Валерьевна — ассистент кафедры медицинской биофизики федерального государственного бюджетного образовательного учреждения высшего образования «Санкт-Петербургский государственный педиатрический медицинский университет» Министерства здравоохранения Российской Федерации; 194100, Санкт-Петербург, Литовская ул., д. 2; врач-рентгенолог отдела лучевой диагностики Городской многопрофильной больницы № 2, 194354, Санкт-Петербург, Россия. e-mail: ellin-ave@yandex.ru, ORCID 0009–0002–6560–6671, SPIN 6799–6535;

Гвоздецкий Антон Николаевич — кандидат медицинских наук, ассистент кафедры психиатрии, федерального государственного бюджетного образовательного учреждения высшего образования «Северо-Западный государственный медицинский университет имени И. И. Мечникова» Министерства здравоохранения Российской Федерации; 191015, Санкт-Петербург, Кирочная ул., д. 41; e-mail: comisora@yandex.ru; ORCID 0000–0001–8045–1220, SPIN 4430–6841;

Алексеев Дмитрий Александрович — кандидат медицинских наук, заведующий отделением — врач-патологоанатом Выборгского межрайонного централизованного патологоанатомического отделения (подразделение государственного бюджетного учреждения здравоохранения «Городское патологоанатомическое бюро»), 194354, Санкт-Петербург, Россия. e-mail: dm_alekseev@bk.ru, ORCID 0000–0001–5912–4663, SPIN 6175–1800;

Александр Владимирович Поздняков — д-р мед. наук, профессор, заведующий отделением лучевой диагностики федерального государственного бюджетного образовательного учреждения высшего образования «Санкт-Петербургский государственный педиатрический медицинский университет» Министерства здравоохранения Российской Федерации; 194100, Санкт-Петербург, Литовская ул., д. 2; e-mail: pozdnyakovalex@yandex.ru, ORCID 0000–0002–1110–066X, SPIN 1000–6408.

Authors' contributions. All authors met the ICMJE authorship criteria. Special contribution: *AVZ, AVP* aided in the concept and plan of the study; *DAA* preparation of histological samples and their digitization *ANG* image postprocessing and mathematical analysis of data, *AVZ, ANG, AVP, DAA* — preparation of the manuscript.

Вклад авторов. Все авторы подтверждают соответствие своего авторства международным критериям ICMJE (все авторы внесли существенный вклад в разработку концепции, проведение исследования и подготовку статьи, прочли и одобрили финальную версию перед публикацией). Наибольший вклад распределен следующим образом: концепция и план исследования — *А. В. Захарова, А. В. Поздняков*; подготовка гистологических образцов и их оцифровка — *Д. А. Алексеев*; постпроцессинг изображений и математический анализ данных — *А. Н. Гвоздецкий*; подготовка рукописи — *А. В. Захарова, А. В. Поздняков, А. Н. Гвоздецкий, Д. А. Алексеев*.

Disclosure: the authors declare that they have no competing interests.

Потенциальный конфликт интересов: авторы заявляют об отсутствии конфликта интересов.

Funding. The authors declare no external funding for the study.

Финансирование. Авторы заявляют об отсутствии внешнего финансирования при проведении исследования.

Adherence to ethical standards: The study was approved by the local ethics committee of St. Petersburg State Pediatric Medical University, protocol number 31/08, dated October 18, 2023. Informed consent was obtained from each patient.

Соответствие принципам этики: Исследование одобрено локальным этические комитетом при Санкт-Петербургском государственном педиатрическом медицинском университете, протокол № 31/08, от 18.10.2023г. Информированное согласие получено от каждого пациента.

Поступила/Received: *08.08.2023*.

Принята к печати/Accepted: *29.11.2023*.

Опубликована/Published: *29.12.2023*.

REFERENCES / ЛИТЕРАТУРА

1. Lee J.H., Koh J., Jeon Y.K. et al. An Integrated Radiologic-Pathologic Understanding of COVID-19 Pneumonia // *Radiology*. 2023. Vol. 306, No. 2. P. e222600. doi: 10.1148/radiol.222600.
2. Kwee T.C., Kwee R.M. Chest CT in COVID-19: What the Radiologist Needs to Know // *RadioGraphics*. 2020. Vol. 40, No. 7. P. 1848–1865. doi: 10.1148/rg.2020200159.
3. Rubin G.D., Ryerson C.J., Haramati L.B. et al. The Role of Chest Imaging in Patient Management during the COVID-19 Pandemic: A Multinational Consensus Statement from the Fleischner Society // *Radiology*. 2020. Vol. 296, No. 1. P. 172–180. doi: 10.1148/radiol.2020201365.
4. Simpson S., Kay F.U., Abbara S. et al. Radiological Society of North America Expert Consensus Document on Reporting Chest CT Findings Related to COVID-19: Endorsed by the Society of Thoracic Radiology, the American College of Radiology, and RSNA // *Radiology: Cardiothoracic Imaging*. 2020. Vol. 2, No. 2. P. e200152. doi: 10.1148/ryct.2020200152.
5. Ai T., Yang Z., Hou H. et al. Correlation of Chest CT and RT-PCR Testing for Coronavirus Disease 2019 (COVID-19) in China: A Report of 1014 Cases // *Radiology*. 2020. Vol. 296, No. 2. P. E32–E40. doi: 10.1148/radiol.2020200642.
6. Suh Y.J., Hong H., Ohana M. et al. Pulmonary Embolism and Deep Vein Thrombosis in COVID-19: A Systematic Review and Meta-Analysis // *Radiology*. 2021. Vol. 298, No. 2. P. E70–E80. doi: 10.1148/radiol.2020203557.
7. Yang R., Li X., Liu H. et al. Chest CT Severity Score: An Imaging Tool for Assessing Severe COVID-19 // *Radiology: Cardiothoracic Imaging*. 2020. Vol. 2, No. 2. P. e200047. doi: 10.1148/ryct.2020200047.
8. Revzin M.V., Raza S, Warshawsky R. et al. Multisystem Imaging Manifestations of COVID-19, Part 1: Viral Pathogenesis and Pulmonary and Vascular System Complications // *RadioGraphics*. 2020. Vol. 40, No. 6. P. 1574–1599. doi: 10.1148/rg.2020200149.
9. Carfì A., Bernabei R, Landi F. et al. Persistent Symptoms in Patients After Acute COVID-19 // *JAMA*. 2020. Vol. 324, No. 6. P. 603. doi: 10.1001/jama.2020.12603.
10. Liu J., Zheng X, Tong Q. et al. Overlapping and discrete aspects of the pathology and pathogenesis of the emerging human pathogenic coronaviruses SARS-CoV, MERS-CoV, and 2019-nCoV // *J. Med. Virol*. 2020. Vol. 92, No. 5. P. 491–494. doi: 10.1002/jmv.25709.
11. John A.E., Joseph C, Jenkins G. et al. COVID-19 and pulmonary fibrosis: A potential role for lung epithelial cells and fibroblasts // *Immunological Reviews*. 2021. Vol. 302, No. 1. P. 228–240. doi: 10.1111/imr.12977.
12. Mohammadi A., Balan I, Yadav S. et al. Post-COVID-19 Pulmonary Fibrosis // *Cureus*. 2022. doi: 10.7759/cureus.22770.
13. Sgalla G., Iovene B., Calvello M. et al. Idiopathic pulmonary fibrosis: pathogenesis and management // *Respir. Res.* 2018. Vol. 19, No. 1. P. 32. doi: 10.1186/s12931-018-0730-2.
14. Tanni S.E., Fabro A.T., De Albuquerque A. et al. Pulmonary fibrosis secondary to COVID-19: a narrative review // *Expert Review of Respiratory Medicine*. 2021. Vol. 15, No. 6. P. 791–803. doi: 10.1080/17476348.2021.1916472.
15. Groff D., Sun A., Ssentongo A.E. et al. Short-term and Long-term Rates of Postacute Sequelae of SARS-CoV-2 Infection: A Systematic Review // *JAMA Netw Open*. 2021. Vol. 4, No. 10. P. e2128568. doi: 10.1001/jamanetworkopen.2021.28568.
16. Liu X., Zhou H, Zhou Y. et al. Risk factors associated with disease severity and length of hospital stay in COVID-19 patients // *Journal of Infection*. 2020. Vol. 81, No. 1. P. e95–e97. doi: 10.1016/j.jinf.2020.04.008.
17. Richeldi L., Collard H.R., Jones M.G. Idiopathic pulmonary fibrosis // *The Lancet*. 2017. Vol. 389, No. 10082. P. 1941–1952. doi: 10.1016/S0140-6736(17)30866-8.

18. Liu F., Mih J.D., Shea B.S. et al. Feedback amplification of fibrosis through matrix stiffening and COX-2 suppression // *Journal of Cell Biology*. 2010. Vol. 190, No. 4. P. 693–706. doi: 10.1083/jcb.201004082.
19. Martinez F.J. Pulmonary Function Testing in Idiopathic Interstitial Pneumonias // *Proceedings of the American Thoracic Society*. 2006. Vol. 3, No. 4. P. 315–321. doi: 10.1513/pats.200602–022TK.
20. Huang C., Huang L., Wang Y. et al. RETRACTED: 6-month consequences of COVID-19 in patients discharged from hospital: a cohort study // *The Lancet*. 2021. Vol. 397, No. 10270. P. 220–232. doi: 10.1016/S0140-6736(20)32656-8.
21. Mylvaganam R.J., Bailey J.I., Sznajder J.I. et al. Recovering from a pandemic: pulmonary fibrosis after SARS-CoV-2 infection // *Eur. Respir. Rev.* 2021. Vol. 30, No. 162. P. 210194. doi: 10.1183/16000617.0194-2021.
22. Nalbandian A., Sehgal K, Gupta A. et al. Post-acute COVID-19 syndrome // *Nat Med*. 2021. Vol. 27, No. 4. P. 601–615. doi: 10.1038/s41591-021-01283-z.
23. Rai D.K., Sharma P., Kumar R. Post COVID-19 pulmonary fibrosis. Is it real threat? // *Indian J Tuberc*. 2021. Vol. 68, No. 3. P. 330–333. doi: 10.1016/j.ijtb.2020.11.003.
24. Mongelli A., Barbi V., Gottardi Zamperla M. et al. Evidence for Biological Age Acceleration and Telomere Shortening in COVID-19 Survivors // *Int. J. Mol. Sci*. 2021. Vol. 22, No. 11. P. 6151. doi: 10.3390/ijms22116151.
25. D'Ettorre G., Gentilini Cacciola E., Santinelli L. et al. COVID-19 sequelae in working age patients: A systematic review // *J. Med. Virol*. 2022. Vol. 94, No. 3. P. 858–868. doi: 10.1002/jmv.27399.
26. Lee J.H., Yim J.-J., Park J. Pulmonary function and chest computed tomography abnormalities 6–12 months after recovery from COVID-19: a systematic review and meta-analysis // *Respir Res*. 2022. Vol. 23, No. 1. P. 233. doi: 10.1186/s12931-022-02163-x.
27. Testa L.C., Jule Y, Lundh L. et al. Automated Digital Quantification of Pulmonary Fibrosis in Human Histopathology Specimens // *Front. Med*. 2021. Vol. 8. P. 607720. doi: 10.3389/fmed.2021.607720.
28. Ashcroft T., Simpson J.M., Timbrell V. Simple method of estimating severity of pulmonary fibrosis on a numerical scale // *Journal of Clinical Pathology*. 1988. Vol. 41, No. 4. P. 467–470. doi: 10.1136/jcp.41.4.467.
29. Cicko S., Grimm M., Ayata K. et al. Uridine supplementation exerts anti-inflammatory and anti-fibrotic effects in an animal model of pulmonary fibrosis // *Respir Res*. 2015. Vol. 16, No. 1. P. 105. doi: 10.3390/biom10111585.
30. De Rudder M., Bouzin C., Nachit M. et al. Automated computerized image analysis for the user-independent evaluation of disease severity in preclinical models of NAFLD/NASH // *Laboratory Investigation*. 2020. Vol. 100, No. 1. P. 147–160. doi: 10.1038/s41374-019-0315-9.
31. Barisoni L., Lafata K.J., Hewitt S.M. et al. Digital pathology and computational image analysis in nephropathology // *Nat. Rev. Nephrol*. 2020. Vol. 16, No. 11. P. 669–685. doi: 10.1038/s41581-020-0321-6.
32. Courtoy G.E., Leclercq I, Froidure A. et al. Digital Image Analysis of Picrosirius Red Staining: A Robust Method for Multi-Organ Fibrosis Quantification and Characterization // *Biomolecules*. 2020. Vol. 10, No. 11. P. 1585. doi: 10.3390/biom10111585.
33. Kinoshita Y., Watanabe K, Ishii H. et al. Proliferation of elastic fibres in idiopathic pulmonary fibrosis: a whole-slide image analysis and comparison with pleuro-parenchymal fibroelastosis // *Histopathology*. 2017. Vol. 71, No. 6. P. 934–942. doi: 10.1111/his.13312.
34. Inui S., Fujikawa A, Jitsu M. et al. Chest CT Findings in Cases from the Cruise Ship Diamond Princess with Coronavirus Disease (COVID-19) // *Radiol. Cardiothorac Imaging*. 2020. Vol. 2, No. 2. P. e200110. doi: 10.1148/ryct.2020200110.
35. Zakharova A.V. Correlation of MR pulmonary perfusion in patients with COVID-19 with quantitative assessment of acute phase CT images // *Diagnostic radiology and radiotherapy*. 2023. Vol. 14. No 3. P. 61-66. https://doi.org/10.22328/2079-5343-2023-14-3-61-66.
36. Cressoni M., Gallazzi E, Chiurazzi C. et al. Limits of normality of quantitative thoracic CT analysis // *Crit Care*. 2013. Vol. 17, No. 3. P. R93. doi: 10.1186/cc12738.
37. Gattinoni L., Chiumello D., Cressoni M. et al. Pulmonary computed tomography and adult respiratory distress syndrome // *Swiss Med Wkly*. 2005. doi: 10.4414/smw.2005.10936.
38. Weller H.I., Van Belleghem S.M., Hiller A.E. et al. Flexible color segmentation of biological images with the R package recolorize: preprint // *Bioinformatics*. 2022. doi: 10.1101/2022.04.03.486906.
39. Wood S.N. Fast Stable Restricted Maximum Likelihood and Marginal Likelihood Estimation of Semiparametric Generalized Linear Models // *Journal of the Royal Statistical Society Series B: Statistical Methodology*. 2011. Vol. 73, No. 1. P. 3–36. doi: 10.1111/j.1467-9868.2010.00749.x.
40. Toussie D., Voutsinas N., Finkelstein M. et al. Clinical and Chest Radiography Features Determine Patient Outcomes in Young and Middle-aged Adults with COVID-19 // *Radiology*. 2020. Vol. 297, No. 1. P. E197–E206. doi: 10.1148/radiol.2020201754.
41. Shen C., Yu N., Cai S. et al. Quantitative computed tomography analysis for stratifying the severity of Coronavirus Disease 2019 // *Journal of Pharmaceutical Analysis*. 2020. Vol. 10, No. 2. P. 123–129. doi: 10.1016/j.jpha.2020.03.004.
42. Caruso D., Zerunian M., Polici M. et al. Diagnostic performance of CT lung severity score and quantitative chest CT for stratification of COVID-19 patients // *Radiol. med*. 2022. Vol. 127, No. 3. P. 309–317. doi: 10.1007/s11547-022-01458-9.
43. Shalmon T., Zerunian M., Polici M. et al. Predefined and data driven CT densitometric features predict critical illness and hospital length of stay in COVID-19 patients // *Sci Rep*. 2022. Vol. 12, No. 1. P. 8143. doi: 10.1038/s41598-022-12311-4.
44. Trias-Sabrià P., Dorca Duch E., Molina-Molina M. et al. Radio-Histological Correlation of Lung Features in Severe COVID-19 Through CT-Scan and Lung Ultrasound Evaluation // *Front. Med*. 2022. Vol. 9. P. 820661. doi: 10.3389/fmed.2022.820661.
45. Henkel M. et al. Lethal COVID-19: Radiologic-Pathologic Correlation of the Lungs // *Radiology: Cardiothoracic Imaging*. 2020. Vol. 2, № 6. P. e200406. doi: 10.1148/ryct.2020200406.
46. Kianzad A., Meijboom L.J., Nossent E.J. et al. COVID-19: Histopathological correlates of imaging patterns on chest computed tomography // *Respirology*. 2021. Vol. 26, No. 9. P. 869–877. doi: 10.1111/resp.14101.
47. Duong-Quy S. et al. Post-COVID-19 Pulmonary Fibrosis: Facts-Challenges and Futures: A Narrative Review // *Pulm Ther*. 2023. P. 1–13. doi: 10.1007/s41030-023-00226-y.